

## A Thieno[3,4-*c*]pyrrole-4,6-dione-Based Donor–Acceptor Polymer Exhibiting High Crystallinity for Photovoltaic Applications

Mao-Chuan Yuan, Mao-Yuan Chiu, Shih-Pin Liu, Chia-Min Chen, and Kung-Hwa Wei\*

Department of Materials Science and Engineering,  
National Chiao Tung University, 30049 Hsinchu, Taiwan, ROC

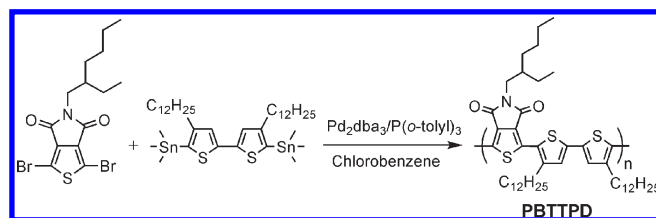
Received July 8, 2010

Revised Manuscript Received August 4, 2010

Polymer solar cells (PSCs) based on bulk heterojunction (BHJ) structures that consist of polymeric donors and fullerene-based acceptors are attracting considerable attention because of their fascinating potential for low-cost, large-area production through solution processing.<sup>1</sup> Because donor–acceptor (D–A) conjugated polymers possess high light-harvesting aptitude, easily tunable optical/electronic properties, and ambipolar charge transporting features, they have been applied extensively to BHJ photovoltaics in the past few years.<sup>2</sup> Specifically, the D–A design concept is the most effective strategy toward harvesting more photons by lowering optical bandgaps while retaining suitable electronic energy levels. In recent years, several efficient D–A polymers have displayed promising potentialities for photovoltaic applications. For instance, electron-deficient units derived from 2,1,3-benzothiadiazole (BT),<sup>3</sup> 2,1,3-benzoxadiazole (BO),<sup>4</sup> 3,6-diaryl-2,5-dihydropyrrolo[3,4-*c*]pyrrole-1,4-dione (DPP),<sup>5</sup> and thieno[3,4-*b*]thiophene-2-carboxylate<sup>6</sup> moieties, when conjugated with various electron-donating units, such as fluorene, carbazole, dithienosilole, and benzodithiophene, have demonstrated distinguished PCEs of up to 7% after systematic optimization.

The electron-deficient thieno[3,4-*c*]pyrrole-4,6-dione (TPD) moiety<sup>7</sup> exhibits a symmetric, rigidly fused, coplanar structure and strong electron-withdrawing properties, which make it a potential system for increasing intramolecular/intermolecular interactions, reducing optical bandgaps, and/or lowering highest occupied molecular orbital (HOMO) energy levels when incorporated into polymeric backbones. Very recently, low-bandgap D–A polymers, comprising TPD and benzodithiophene moieties, were prepared that featured relatively low-lying HOMO energy levels (–5.43 to –5.57 eV), high open-circuit voltages ( $V_{oc}$ , up to 0.89 V), and prominent PCEs (4–6%).<sup>8</sup> When designing new efficient D–A polymers, it is important to select suitable electron donors as well as acceptors by taking into consideration their spectral absorption ranges and electronic energy levels. Furthermore, the development of new D–A polymers exhibiting crystalline characteristics can lead to significantly enhanced charge transporting mobilities in the active layers of the devices. Several p-type conjugated polymers containing the symmetric bi(dodecyl)-thiophene unit exhibit crystalline characteristics and high hole mobilities when used in organic field effect transistors.<sup>9</sup> Considering not only the electronic energy level but also the hole mobility, we prepared a new D–A polymer, PBTTTPD, wherein the electron-withdrawing TPD unit was conjugated with the symmetrical electron-donating bi(dodecyl)thiophene unit to provide crystalline characteristics and a low-lying HOMO energy level, resulting from the combination of the rigidly fused TPD moiety and the symmetrical bi(dodecyl)thiophene units. Because of these desirable

Scheme 1. Synthetic Route and Structure of PBTTTPD



features, we expected PBTTTPD to exhibit good hole mobility and high values of  $V_{oc}$  when used in photovoltaic applications.

We prepared PBTTTPD (Scheme 1) through Stille polymerization of the monomers 1,3-dibromo-5-ethylhexylthieno[3,4-*c*]pyrrole-4,6-dione (M1) and 4,4'-didocecyl-5,5'-bis(trimethylstannyl)-2,2'-bithiophene (M2) using tris(dibenzylideneacetone)dipalladium/tri(*o*-tolyl)phosphine [ $\text{Pd}_2\text{dba}_3/\text{P}(o\text{-tolyl})_3$ ] as the catalyst. The branched 2-ethylhexyl chain of the TPD moiety was present to promote the solubility of the polymer. The number-average molecular weight of PBTTTPD was  $9.7 \text{ kg mol}^{-1}$ , with a polydispersity of 1.4, as determined through gel permeation chromatography (GPC) using chloroform as the eluent. This polymer was readily soluble in hot chlorinated solvents, namely chloroform, chlorobenzene, and dichlorobenzene. PBTTTPD exhibited good thermal stability, with its decomposition temperature ( $T_d$ ) greater than  $400 \text{ }^\circ\text{C}$ , as measured using thermogravimetric analysis (TGA; Supporting Information, Figure S1). We investigated the thermal behavior of this polymer using differential scanning calorimetry (DSC), which revealed two distinct peaks—a melting point at  $297 \text{ }^\circ\text{C}$  and a crystallization point at  $268 \text{ }^\circ\text{C}$ —but no glass transition (Supporting Information, Figure S2). The presence of the pronounced crystallization peak indicated that PBTTTPD had a strong inclination to crystallize, which we further confirmed from its film's grazing-incidence X-ray diffraction pattern (Figure 1a). In Figure 1a, the (100), (200), and (300) diffraction peaks for PBTTTPD are at  $3.4^\circ$ ,  $6.8^\circ$ , and  $10.2^\circ$ , respectively, indicating a highly ordered structure along with a *d*-spacing of  $26 \text{ \AA}$  that is ascribable to the interchain distance separated by the alkyl side chains; the broad feature at  $24.6^\circ$ , corresponding to a short distance of  $3.6 \text{ \AA}$ , is assigned to the facial  $\pi$ – $\pi$  stacking between polymeric backbones; such high crystallinity suggested that PBTTTPD would exhibit good carrier mobility when applied in PSCs.

Figure 1b presents absorption spectra of PBTTTPD in dilute chloroform solution and in the solid state. In solution, the polymer exhibited an absorption signal at  $468 \text{ nm}$ , which we assign to internal charge transfer between the TPD acceptor and the bithiophene donor.<sup>7a</sup> The absorption maximum of the solid state polymer appeared at  $572 \text{ nm}$ —a significant red shift of  $104 \text{ nm}$  relative to that in solution, indicating that considerably strong intermolecular interactions existed in the solid film. Additionally, a vibronic shoulder at  $628 \text{ nm}$  implies an ordered arrangement of PBTTTPD in the solid film, with strong  $\pi$ – $\pi$  stacking between the polymeric backbones, a feature that also appears in regioregular poly(3-hexylthiophene). The optical bandgap of PBTTTPD, estimated from the onset of absorption in the solid film, was  $1.82 \text{ eV}$ ; this value is less than that of P3HT ( $1.91 \text{ eV}$ )<sup>2a</sup> because of the presence of the electron-accepting TPD moiety in the polymer main chain; accordingly, we expected that PBTTTPD would harvest more photons relative to P3HT.

Figure S3 presents the redox behavior of the polymer (see Supporting Information). On the basis of the onset potentials, we

\*Corresponding author. E-mail: khwei@mail.nctu.edu.tw.

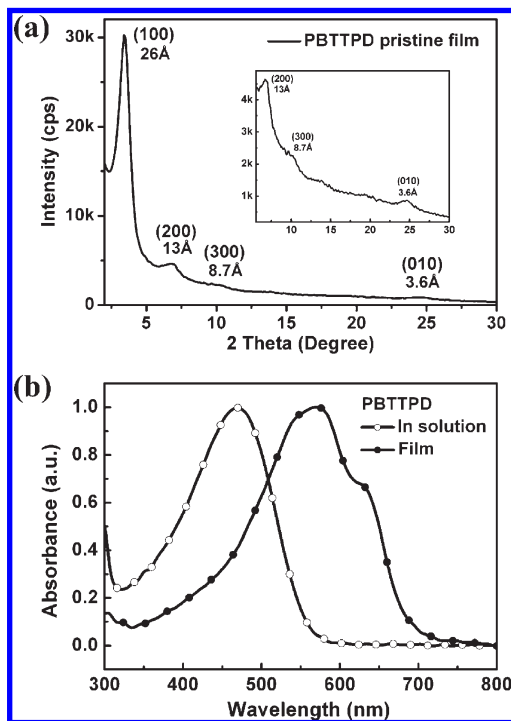


**Figure 1.** (a) X-ray diffraction pattern of the pristine PBTTTPD film. (b) UV-vis absorption spectra of PBTTTPD in dilute  $\text{CHCl}_3$  ( $1 \times 10^{-5}$  M) and as a solid film.

estimated the HOMO and lowest unoccupied molecular orbital (LUMO) energy levels of PBTTTPD to be  $-5.56$  and  $-3.10$  eV, respectively. The presence of the TPD moiety provided the polymer with a low-lying HOMO energy level, indicating that the moiety is strongly electron-withdrawing; moreover, the HOMO energy level of PBTTTPD ( $-5.56$  eV) was located significantly below  $-5.2$  eV, implying good stability against oxidation in air,<sup>4a,10</sup> a property that would enhance device stability. The electrochemical bandgap of PBTTTPD, estimated from the difference between the onset potentials for oxidation and reduction, was 2.46 eV, a value that is somewhat larger than its optical bandgap (1.82 eV); similar phenomena have been observed in studies of other D-A polymers,<sup>3a,8b,11</sup> presumably resulting from the interface barrier for charge injection.<sup>11a,12</sup> Moreover, the hole mobility of the pristine PBTTTPD and PBTTTPD:PCBM (1:1.5, w/w) film was  $1 \times 10^{-4}$  and  $8 \times 10^{-5} \text{ cm}^2 \text{ V}^{-1} \text{ s}^{-1}$ , respectively, as determined using the space-charge-limited current (SCLC) method (see Supporting Information), presumably because its crystalline characteristics promoted charge transport in the device.

Next, we investigated the photovoltaic properties of PBTTTPD in BHJ solar cells having the sandwich structure indium tin oxide (ITO)/poly(3,4-ethylenedioxythiophene):poly(styrenesulfonate) (PEDOT:PSS)/PBTTTPD:[6,6]-phenyl- $\text{C}_{61}$ -butyric acid methyl ester (PCBM)/Al, where the photoactive layers, spin-coated from the chloroform solutions with various blend compositions, had thicknesses in the range 90–100 nm. Figure 2 presents the current density–voltage curves of the BHJ solar cells with different active layer compositions in the dark and under the illumination; Table 1 summarizes the data. The optimal device efficiency was obtained from the device with an active layer that comprised a blend of PBTTTPD and PCBM at a weight ratio of 1:1.5; this device displayed a value of  $V_{\text{oc}}$  of 0.95 V, a short-circuit current density ( $J_{\text{sc}}$ ) of  $8.02 \text{ mA cm}^{-2}$ , a fill factor of 0.62, and a resulting PCE of 4.7%. Because the value of  $V_{\text{oc}}$  is proportional to the difference between the HOMO energy level of the polymer and the LUMO energy level of PCBM,<sup>1c</sup> we anticipated that the PBTTTPD blend would generate a high value of  $V_{\text{oc}}$  because of its

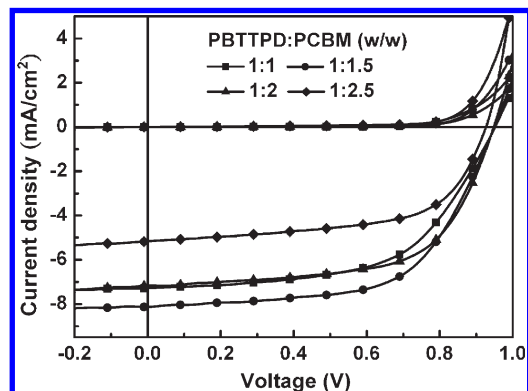


**Figure 2.** Current density–voltage ( $J$ – $V$ ) characteristics of PSCs incorporating the PBTTTPD:PCBM blend at various weight ratios (w/w).

**Table 1. Photovoltaic Properties of Polymer Solar Cells Incorporating PBTTTPD:PCBM Blends Prepared at Various Weight Ratios**

ratio (w/w)	$V_{\text{oc}}$ (V)	$J_{\text{sc}}$ ( $\text{mA cm}^{-2}$ )	FF	PCE (%)
1:1	0.95	7.23	58	4.0
1:1.5	0.95	8.02	62	4.7
1:2	0.95	7.16	63	4.3
1:2.5	0.93	5.12	61	2.9

low-lying HOMO energy level. Figure S5 presents the external quantum efficiency (EQE) curves of the devices, where the active layers consisted of PBTTTPD:PCBM at various weight ratios. These devices exhibited broad EQE responses from 300 to 700 nm, which resulted from the absorption of PBTTTPD. The best EQE performance is obtained from the device with an active layer of 1:1.5 (w/w) PBTTTPD:PCBM which displayed a maximum intensity of 50% at 560 nm. The theoretical  $J_{\text{sc}}$  calculated by integrating the EQE curve of this device is  $7.70 \text{ mA cm}^{-2}$ , which is in reasonable agreement with the  $J_{\text{sc}}$  of  $8.02 \text{ mA cm}^{-2}$  from the  $J$ – $V$  measurement. Furthermore, we used atomic force microscopy (AFM) to determine the morphology of the PBTTTPD:PCBM (1:1.5, w/w) blend (Supporting Information, Figure S6). The height and phase images of the blend revealed a moderately homogeneous surface and no significant phase segregation, with a room-mean-square roughness of 2.5 nm, indicating a decent morphology of the PBTTTPD:PCBM blend, thereby leading to good device performance.

In conclusion, we have used Stille polymerization to prepare the thieno[3,4-*c*]pyrrole-4,6-dione (TPD)-based polymer PBTTTPD, which features excellent thermal stability, crystalline characteristics, and a low-lying HOMO energy level; these desirable properties mean that PBTTTPD has promising potential for application in polymer solar cells. Through devices' composition optimization, a device incorporating the PBTTTPD/PCBM blend at a weight ratio of 1:1.5 displayed an open-circuit voltage of 0.95 V and, therefore, a PCE of 4.7%.

**Acknowledgment.** We thank the National Science Council for financial support through project NSC 98-2120-M-009-006.

**Supporting Information Available:** Experimental details; device fabrication and characterization; TGA, DSC, and CV of the polymer; AFM images of the polymer blend. This material is available free of charge via the Internet at <http://pubs.acs.org>.

## References and Notes

- (1) (a) Coakley, K. M.; McGehee, M. D. *Chem. Mater.* **2004**, *16*, 4533. (b) Thompson, B. C.; Fréchet, J. M. J. *Angew. Chem., Int. Ed.* **2008**, *47*, 58–77. (c) Dennler, G.; Scharber, M. C.; Brabec, C. J. *Adv. Mater.* **2009**, *21*, 1323.

- (2) (a) Chang, Y.-T.; Hsu, S.-L.; Chen, G.-Y.; Su, M.-H.; Singh, T. A.; Diau, E. W.-G.; Wei, K.-H. *Adv. Funct. Mater.* **2008**, *18*, 2356. (b) Huang, F.; Chen, K.-S.; Yip, H.-L.; Hau, S. K.; Acton, O.; Zhang, Y.; Luo, J.; Jen, A. K.-Y. *J. Am. Chem. Soc.* **2009**, *131*, 13886. (c) Chang, Y.-T.; Hsu, S.-L.; Su, M.-H.; Wei, K.-H. *Adv. Mater.* **2009**, *21*, 2093. (d) Wu, P.-T.; Bull, T.; Kim, F. S.; Luscombe, C. K.; Jenekhe, S. A. *Macromolecules* **2009**, *42*, 671. (e) Zhang, M.; Fan, H.; Guo, X.; He, Y.; Zhang, Z.; Min, J.; Zhang, J.; Zhao, G.; Zhan, X.; Li, Y. *Macromolecules* **2010**, *43*, 5706. (f) Yuan, M.-C.; Chiu, M.-Y.; Chiang, C.-M.; Wei, K.-H. *Macromolecules* **2010**, *43*, 6270.
- (3) (a) Hou, J.; Chen, H.-Y.; Zhang, S.; Li, G.; Yang, Y. *J. Am. Chem. Soc.* **2008**, *130*, 16144. (b) Baek, N. S.; Hau, S. K.; Yip, H.-L.; Acton, O.; Chen, K.-S.; Jen, A. K.-Y. *Chem. Mater.* **2008**, *20*, 5734. (c) Park, S. H.; Roy, A.; Beaupré, S.; Cho, S.; Coates, N.; Moon, J. S.; Moses, D.; Leclerc, M.; Lee, K.; Heeger, A. J. *Nature Photonics* **2009**, *3*, 297. (d) Price, S. C.; Stuart, A. C.; You, W. *Macromolecules* **2010**, *43*, 4609.
- (4) (a) Blouin, N.; Michaud, A.; Gendron, D.; Wakim, S.; Blair, E.; Neagu-Plesu, R.; Belletête, M.; Durocher, G.; Tao, Y.; Leclerc, M. *J. Am. Chem. Soc.* **2008**, *130*, 732. (b) Bijleveld, J. C.; Shahid, M.; Gilot, J.; Wienk, M. M.; Janssen, R. A. J. *Adv. Funct. Mater.* **2009**, *19*, 3262. (c) Hoven, C. V.; Dang, X.-D.; Coffin, R. C.; Peet, J.; Nguyen, T.-Q.; Bazan, G. C. *Adv. Mater.* **2010**, *22*, E63.
- (5) (a) Bijleveld, J. C.; Zoombelt, A. P.; Mathijssen, S. G. J.; Wienk, M. M.; Turbiez, M.; de Leeuw, D. M.; Janssen, R. A. J. *J. Am. Chem. Soc.* **2009**, *131*, 16616. (b) Zhou, E.; Wei, Q.; Yamakawa, S.; Zhang, Y.; Tajima, K.; Yang, C.; Hashimoto, K. *Macromolecules* **2010**, *43*, 821. (c) Chen, G.-Y.; Chiang, C.-M.; Kekuda, D.; Lan, S.-C.; Chu, C.-W.; Wei, K.-H. *J. Polym. Sci., Part A: Polym. Chem.* **2010**, *48*, 1669.
- (6) (a) Liang, Y.; Wu, Y.; Feng, D.; Tsai, S.-T.; Son, H.-J.; Li, G.; Yu, L. *J. Am. Chem. Soc.* **2009**, *131*, 56. (b) Chen, H.-Y.; Hou, J.; Zhang, S.; Liang, Y.; Yang, G.; Yang, Y.; Yu, L.; Wu, Y.; Li, G. *Nature Photonics* **2009**, *3*, 649. (c) Liang, Y.; Xu, Z.; Xia, J.; Tsai, S.-T.; Wu, Y.; Li, G.; Ray, C.; Yu, L. *Adv. Mater.* **2010**, *22*, E135.
- (7) (a) Zhang, Q. T.; Tour, J. M. J. *J. Am. Chem. Soc.* **1998**, *120*, 5355. (b) Pomerantz, M.; Amarasekara, A. S. *Synth. Met.* **2003**, *135–136*, 257. (c) Nielsen, C. B.; Bjørnholm, T. *Org. Lett.* **2004**, *6*, 3381.
- (8) (a) Zou, Y.; Najari, A.; Berrouard, P.; Beaupré, S.; Aïch, B. R.; Tao, Y.; Leclerc, M. *J. Am. Chem. Soc.* **2010**, *132*, 5330. (b) Zhang, Y.; Hau, S. K.; Yip, H.-L.; Sun, Y.; Acton, O.; Jen, A. K.-Y. *Chem. Mater.* **2010**, *22*, 2696. (c) Piliago, C.; Holcombe, T. W.; Douglas, J. D.; Woo, C. H.; Beaujuge, P. M.; Fréchet, J. M. J. *J. Am. Chem. Soc.* **2010**, *132*, 7595.
- (9) (a) Osaka, I.; Sauvé, G.; Zhang, R.; Kowalewski, T.; McCullough, R. D. *Adv. Mater.* **2007**, *19*, 4160. (b) Li, J.; Qin, F.; Li, C. M.; Bao, Q.; Chan-Park, M. B.; Zhang, W.; Qin, J.; Ong, B. S. *Chem. Mater.* **2008**, *20*, 2057. (c) Rieger, R.; Beckmann, D.; Pisula, W.; Steffen, W.; Kastler, M.; Müllen, K. *Adv. Mater.* **2010**, *22*, 83.
- (10) de Leeuw, D. M.; Simenon, M. M. J.; Brown, A. R.; Einerhand, R. E. F. *Synth. Met.* **1997**, *87*, 53.
- (11) (a) Wu, P.-T.; Kim, F. S.; Champion, R. D.; Jenekhe, S. A. *Macromolecules* **2008**, *41*, 7021. (b) Hou, J.; Park, M.-H.; Zhang, S.; Yao, Y.; Chen, L.-M.; Li, J.-H.; Yang, Y. *Macromolecules* **2008**, *41*, 6012.
- (12) Chen, Z.-K.; Huang, W.; Wang, L.-H.; Kang, E.-T.; Chen, B. J.; Lee, C. S.; Lee, S. T. *Macromolecules* **2000**, *33*, 9015.